Ewing's Sarcoma EWS protein regulates skeletogenesis by modulation of SOX9

By

Christopher Michael Merkes

Submitted to the graduate degree program in Molecular Biosciences and the Graduate Faculty of the University of Kansas in partial fulfillment of the requirements for the degree of Master of Arts.

_____

Chairperson: Dr. Mizuki Azuma

_____

Dr. Erik Lundquist

_____

Dr. Stuart Macdonald

Date Defended: 12-April, 2013

The Thesis Committee for Christopher Michael Merkes

certifies that this is the approved version of the following thesis:

Ewing's Sarcoma EWS Protein regulates skeletogenesis by modulation of SOX9

_____

Chairperson: Dr. Mizuki Azuma

Date approved: 12-April, 2013

ABSTRACT

Ewing sarcoma is the second most common form of bone cancer in adolescents, characterized by the presence of an aberrant chimeric fusion gene EWS/FLI1. Wildtype EWS has been proposed to play a role in splicing and transcription. Currently, how these functions affect early developmental stages is unknown. To elucidate the function of EWS in early development, we analyzed an *ewsa* zebrafish mutant line originally isolated from an insertional mutagenesis method**.** We generated a Maternal Zygotic (MZ) *ewsa/ewsa* line because *ewsa/wt* and *ewsa/ewsa* zebrafish appear to be normal and are fertile. Alizarin Red staining revealed that there are skeletal formation defects in the lower jaw with an aberrant angle and position of the dentary and basihyal bones in adult MZ *ewsa/ewsa* mutants. Alcian blue staining revealed that the MZ *ewsa/ewsa* mutation leads to craniofacial defects with higher numbers of smaller cells with disorganized polarization compared to *wt/wt* zebrafish at four days post fertilization (dpf). In addition, there were reduced intervertebral discs and asymmetrical vertebrae leading to curved spines in MZ *ewsa/ewsa* mutants. MZ *ewsa/ewsa* mutants display disorganized alignment of Sox9 expressing neural crest cells at 27hpf. Because both craniofacial skeletons and vertebrae arise from Sox9 expressing cells, we hypothesized that EWS interacts with Sox9 and modulates the transcriptional regulation activity of Sox9. Co-immunoprecipitation (IP) experiment revealed that EWS interacts with SOX9. Furthermore, qPCR analysis identified that known SOX9 target genes are either upregulated (*ctgfa, ctgfb, col2a1a, col2a1b*) or downregulated (*sox5, nog1, nog2, bmp4*) in MZ *ewsa/ewsa* mutants compared to *wt/wt* zebrafish embryos. This is the first evidence for a tissue specific role of EWS in skeletogenesis and suggests a novel mechanism by which Sox9 transcriptional regulation is modulated as it directs endochondral bone and cartilage development.

ACKNOWLEDGEMENTS

I would like to thank my committee (Dr. Mizuki Azuma, Dr. Erik Lundquist, and Dr. Stuart Macdonald) for their support and guidance while pursuing this research. I would like to thank Dr. Yoshiaki Azuma for use of reagents and equipment in my experiments. I would like to thank Nicole Wilder and Timothy Turkalo for assistance with experiments. I would also like to thank K-INBRE, COBRE, and The Massman Family Ewing Sarcoma Research Fund for funding support for this research.

TABLE OF CONTENTS

INTRODUCTION

EWS was originally discovered in Ewing's Sarcoma, the second most common bone cancer in adolescents and young adults. EWS was found as a part of an aberrant fusion gene containing the sequence coding N-terminal transactivation domain of EWS fused to the C-terminal domains of an ETS transcription factor FLI1 (Delattre, 1994). Expression of the EWS-FLI1 fusion protein has been shown to lead to altered transcription and splicing (Tirode, 2007; Sanchez, 2008), and it has further been shown to interact directly with EWS antimorphically (Embree, 2009). EWS has been implicated to have roles in transcription and splicing (Rossow, 2001; Araya, 2003, 2005; Li, 2010; Sanchez, 2008). Its knockdown has further been shown to result in mitotic defects and senescence (Azuma, 2007; Cho, 2011). An EWS knockdown study in mice (Li, 2007) revealed that homozygous $EWS^{-/-}$ mice are embryonic lethal in 129SvEv and C57BL/6 backgrounds. Whereas, runted homozygous $EWS^{-/-}$ mice died soon after birth and displayed reduced thymi and spleens in a black swiss background. Although, the cause of death was undetermined, it suggests that EWS regulates early developmental stages. To address this, we utilized an ews zebrafish mutant, because they spawn eggs *ex vivo*, and this allows us to observe their development from the one cell stage.

We suspected EWS may have a role in skeletal development, because Ewing's Sarcoma is a bone related cancer and EWS knockout mice are smaller in size compared to wild type littermates (Li, 2007). Knockdown or knockout mutants of genes that regulate skeletogenesis (e.g. *pax1/pax9* in mice, *sox5/sox6* in mice, *sox9* in mice, *fzd7* in chickens, *fam20b* and *xylt1* in zebrafish) often result in a reduction of appendages, body regions, or the entire animal overall (Peters, 1999; Bi, 2001; Akiyama, 2002; Li, 2009; Eames, 2011; Henry, 2012). Skeletogenesis is a significant process, because skeletal elements shape and provide support to the body, allow locomotion, and protect vital tissues from damage. Skeletal elements

originate from mesenchymal cells which migrate to the proper regions followed by condensation. Skeletal differentiation follows two mechanisms: intramembranous ossification or endochondral ossification (reviewed in Karsenty, 2002). Intramembranous ossification is a differentiation process during which condensed mesenchymal cells differentiate directly into osteoblasts, osteocytes, and osteoclasts. While endochondral ossification is a process during which condensed mesenchymal cells will first differentiate into chondrocytes, secrete extracellular matrix, and form cartilages that grow by convergent extension.

Craniofacial skeletons are derived from neural crest cells. During neurulation, cells at the lateral edges of the neural plate will form the dorsalmost region of the neural tube and attain neural crest specification. Neural crest cells are a unique multipotent cell population that migrates long distances to form multiple lineages including craniofacial skeleton, pigment cells, and peripheral nerves. After neural closure, cranial neural crest cells will migrate ventrally to form the pharyngeal arches. These arch cells will receive patterning signals from dlx gene expression (Talbot, 2010) and migrate further to form mesenchymal condensations which will give rise to the craniofacial cartilages destined to become endochondral bones of the head (Noden, 1983; Kague, 2012). Later in development, vertebrae are formed by sclerotomes and notochord. After somitogenesis is completed, somitic cells differentiate into dermomyotome and sclerotome. Sclerotomal induction is mediated by *shh, bmp,* and *noggin* cues received from the notochord and neural tube (Fan, 1994; Johnson, 1994; McMahon, 1998; Watanabe, 1998). Sclerotomal cells then migrate around the notochord and undergo resegmentation (Remak, 1855; von Ebner, 1888; Bagnall, 1988; Aoyama, 2000). As a result of sclerotomal resegmentation, the rostral half of somites form the caudal half of anterior vertebra and the caudal half of somites form the rostral half of the adjacent posterior vertebra. After sclerotomal cells surround the notochord and are resegmented, they undergo endochondral ossification and form the vertebrae (Arratia, 2001).

Importantly, differentiation of craniofacial skeletons and vertebrae are both regulated by the transcription factor SOX9 (Akiyama, 2002; Cheung, 2003). To undergo endochondral ossification, craniofacial prechondrocytes and vertebral condensations require Sox9 activity to regulate their proliferation, maturation, and expression of extra cellular matrix proteins such as aggrecan and collagen type II α 1 (Lefebvre, 1997; Bi, 1999; Akiyama, 2002). Sox9 mutations are associated with campomelic dysplasia. Here, we demonstrate that EWS interacts with SOX9 and regulates skeletogenesis. The *ewsa* knockout zebrafish mutant was utilized, and we show it leads to craniofacial and axial skeleton defects. This is the first demonstration of a role of EWS in skeletogenesis, and it may contribute to understanding the mechanism for regulation of SOX9 and ultimately to Ewing's Sarcoma formation.

MATERIALS AND METHODS

Aquaculture

Zebrafish families were bred and maintained at 28.5^{o}C using an automatic filtration system from Aquatic Eco-Systems Inc, and embryos were staged as previously described (Kimmel et al, 1995). The wild type line used was the Oregon AB line. The *ewsa/ewsa* line was generated by insertional mutagenesis by Znomics Inc, and is maintained as a Maternal Zygotic (MZ) line in our system.

Alizarin red staining

Zebrafish were stained with alizarin red as previously described (Javidan and Schilling, 2004). Fish were anesthetized with 0.04% Tricaine Methanesulfonate (MS222) and fixed overnight at 4^{o}C in 4% paraformaldehyde. Viscera were removed surgically, and pigment was ablated by treatment with 3% H_2O_2 in 1% KOH. Tissue was permeabilized with acetone at room temperature and cleared with 0.05% trypsin at 37^{o}C. Cleared specimens were stained with 0.05% alizarin red dissolved in 1% KOH, destained with 1% KOH, and stored in glycerol.

Images were taken with a Leica DFC320 camera mounted on a Leica MZ FLIII dissecting microscope.

Alcian blue staining

Embryos were stained with alcian blue as previously described (Walker, 2007; Neuhauss, 1996) with minor modifications. Embryos were anesthetized with MS222 and fixed overnight at 4^{o}C in 4% paraformaldehyde. Pigment was ablated by treatment with 10% H_2O_2 in 0.1% KOH. Embryos were equilibrated to acidified ethanol (5% HCl, 70% ethanol) before staining overnight in 0.1% alcian blue dissolved in acidified ethanol. Specimens were then washed extensively with acidified ethanol and dehydrated by ethanol series before transferring to glycerol. Double stained embryos were treated the same way, but without any acid using a 0.02% alcian blue / 0.005% alizarin red solution in 60 mM $MgCl_2$ / 70% ethanol. Microdissections and flat mounting were performed using tungsten needles as described (Javidan and Schilling, 2004). Images were taken with a Leica DFC320 camera mounted on a Leica MZ FLIII dissecting microscope.

Immunohistochemistry

Embryos were visualized as previously described (Azuma et al, 2007). Fixed embryos were permeabilized with methanol at -20^{o}C overnight, digested with 0.01% trypsin, and then blocked with blocking solution (10% fetal bovine serum, 1% dimethyl sulfoxide, 0.1% triton x-100). Primary antibodies were applied overnight at 4^{o}C; embryos were washed thoroughly; and secondary antibodies were applied overnight at 4^{o}C. Embryos were then washed thoroughly again, equilibrated to 50% glycerol, and stored in 100% glycerol. We used a mouse monoclonal anti-collagen II primary antibody (II-II6B3 from Developmental Studies Hybridoma Bank at University of Iowa) diluted 1:250 and anti-mouse Alexa 594 secondary antibody diluted 1:250 to visualize collagen II. We used a mouse monoclonal anti-sox9 primary antibody (ab76997 from

abcam) diluted 1:250 and anti-mouse Alexa 594 secondary antibody diluted 1:250 to visualize sox9. Images were taken with a Leica DFC320 camera mounted on a Leica MZ FLIII dissecting microscope.

In situ hybridization

In situ hybridization was performed as previously described (Azuma et al, 2006). Fixed embryos were permeabilized in methanol at -20^{o}C overnight then washed in PBS. Embryos were then equilibrated in HYB buffer at 60^{o}C for 3 hours. Embryos were then hybridized overnight at 60^{o}C with antisense RNA generated with T7 RNA polymerase and DIG-labeled dUTP. Embryos were then treated with anti-DIG antibodies conjugated with alkaline phosphatase (AP) overnight at 4^{o}C. After equilibration with AP buffer, signal was developed with BM Purple, and then embryos were fixed again in 4% paraformaldehyde at room temperature for 10 minutes.

Co-immunoprecipitation

HeLa cells were plated and grown to 95% confluency in 9 cm dishes and then incubated at 35^{o}C for 16 hours in optimem media containing 10% fetal bovine serum. Matching dishes also contained either no DNA (untransfected), 26.4 μg of a control plasmid having the Sox9 coding sequence cut out (empty vector), or 26.4 μg of a Sox9 expression plasmid (sox9 experimental). Transfection DNA was incubated at room temperature in 3.3 mL optimem with 53 μL of Lipofectamine2000 reagent (Invitrogen cat# 11668-019) prior to applying it to cells. After transfection, cells were then washed twice with phosphate buffered saline (PBS) and lysed in 3 mL of lysis buffer (2 mM Tris pH 7.6, 1% Triton X-100, 1 mM EDTA, 150 mM NaCl) containing protease inhibitors: leupepstatin, pepstatin, chymotrypsin, and AEBSF. Lysates were incubated on ice for 20 minutes before pelleting at 12,000 rpm for 1 minute. 50 μL aliquots of the supernatant were collected to represent the input fraction. 900 μL of the supernatant was

applied to antibody crosslinked magnetic dynabeads. Paired precipitations were done with each sample using an anti-mouse IgG nonspecific control and anti-FLAG antibodies (Agilent Ab 200472-21). The precipitations were rotated at 4°C for 1 hour, and then washed 3 times with lysis buffer (rotating at 4°C) for 20 minutes each wash. The precipitates were boiled in SDS sample buffer and subjected to SDS-PAGE alongside the input fractions. Presence of EWS and Sox9 were detected by western blot using anti-EWS (SantaCruz sc-48404) and anti-FLAG (Agilent Ab 200472-21) antibodies respectively. The western blots were visualized by anti-mouse antibodies conjugated to horseradish peroxidase and subjected to FEMTO ECL substrate (Pierce cat# 34095).

qPCR

Total RNA was isolated from whole embryos flash frozen at 27 hpf using the RNeasy Mini Kit (Qiagen cat# 74104) following the manufacturer's protocol and using the optional on column DNase digestion (Qiagen cat# 79254). Embyos were mechanically dissociated by repeatedly drawing them into and expelling them from a syringe with buffer RLT. Samples were centrifuged at max RPM for 3 minutes and the supernatant was mixed with 60% volume of ethanol then loaded onto spin columns. The columns were washed once, and then treated with DNase at 37°C for 30 minutes. The columns were washed once more with buffer RW1, 3 times with buffer RPE (2 washes included 5 minute incubations at room temperature), and then eluted with water. RNA was quantified using an Eppendorf BioPhotometer, and 1 μg was used to make 20 μL of cDNA or reverse transcriptase (RT) negative paired controls. Reaction tubes contained 10 U/μL M-MLV RT (Invitrogen cat# 18080-093), 1x Fist-Strand Buffer, 50 mM DTT, 0.5 mM dNTPs, and 2.5 μM dT oligos. RNA was denatured at 65°C for 5 minutes with dT oligos and dNTPs, then the buffer, DTT, and RT were added. The reaction was incubated at room temperature for 5 minutes, 50°C for 1 hour, 70°C for 15 minutes, and put on ice before use in qPCR analysis. 1 μL of cDNA, RT negative control, or water (no template control) was used in

20 μL reactions with 1x Power SYBR Green PCR Master-Mix (Applied Biosystems part# 4367659) and 0.9 μM forward and reverse primers (table S2). 96-well plates were run on a StepOnePlus Real-Time PCR System (Applied Biosystems), and cycle thresholds were determined using the manufacturer's software. Relative expression levels were calculated by the comparative $\Delta\Delta C_T$ method previously described (Schmittgen and Livak, 2008) using GAPDH mRNA levels as the endogenous control.

RESULTS

MZ *ewsa/ewsa* mutation in zebrafish leads to craniofacial bone developmental defects

Previous reports have shown that there were not any $EWS^{-/-}$ homozygous mice that managed to survive until birth in 129SvEv or C57BL/6 inbred mouse backgrounds. On the other hand, $EWS^{-/-}$ knockout in black swiss outbred mice exhibit postnatal lethality with 90% of newborns dying before weaning and only one of 18 surviving to postnatal day 21 (Li, 2007). The surviving homozygous $EWS^{-/-}$ mice were runted with disproportionately small thymi and spleens. Cause of death is yet to be determined. These results indicate that Ews plays a significant role during development. To address the role of Ews during development, we utilized a zebrafish model because they spawn eggs *ex vivo*, and this allows us to observe their development beginning at the one cell stage. Due to the genome duplication event before the teleost radiation (Amores, 1998; Postlethwait, 1998), there are two zebrafish homologues of human *ews*, *ewsa* and *ewsb* (Azuma, 2007). To elucidate the role of Ewsa, we obtained an *ewsa* zebrafish mutant line originally isolated in an insertional mutagenesis screen (Znomics Inc.). A retroviral vector was integrated immediately after the third amino acid from the start codon. We generated a peptide antibody that recognized Ewsa and Ewsb due conserved sequences of the antigen sites. Using this antibody, we performed a western blot using the lysates extracted from 24 hpf *wt/wt* and *ewsa/ewsa* embryos. As a result, the Ewsa protein was

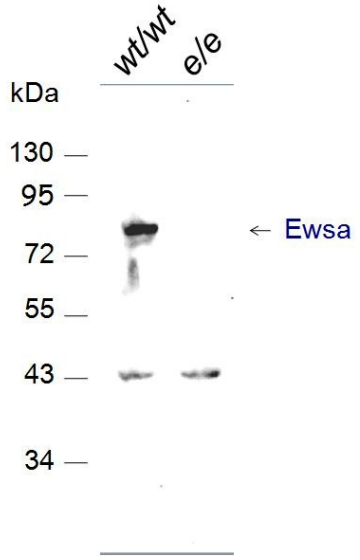

Figure 1: *ewsa/ewsa* mutants are Ewsa protein null mutants

Western blot of zebrafish cell lysates from *wildtype/wildtype (wt/wt)* and *ewsa/ewsa (e/e)* embryos that was probed with an anti-Ewsa antibody raised against zebrafish Ewsa showing that MZ *ewsa/ewsa* mutants are protein null.

absent in the protein extracts from *ewsa/ewsa* mutants confirming that it is a protein null mutant for Ewsa (figure 1).

Heterozygous *ewsa/wt* and a subset of homozygous *ewsa/ewsa* zebrafish appear to be normal and are fertile. We further generated a maternal-zygotic (MZ) *ewsa/ewsa* mutant line by intercrossing zygotic *ewsa/ewsa* homozygous mutants. Unlike the $EWS^{-/-}$ mice which are infertile with high postnatal lethality (Li, 2007), the *ewsa/ewsa* zebrafish mutants survive until adulthood and are fertile. The phenotypic discrepancy between $EWS^{-/-}$ mice and *ewsa/ewsa* mutant zebrafish lines is likely due to redundant expression of the *ewsb* gene in zebrafish. The MZ *ewsa/ewsa* mutants develop normal morphology including a straight notochord and somites at the 17 somite stage (figure S1C). To examine whether specification is affected during development, *in situ* hybridizations were performed in *wt/wt* and MZ *ewsa/ewsa* mutant embryos at 27 hours post fertilization (hpf). Three probes for tissue specific genes, *ntl* (notochord), *eng3* (midbrain-hindbrain boundary), and *krox20* (rhombomere 2 and 4 in hindbrain) did not exhibit any significant differences between *wt/wt* and MZ *ewsa/ewsa* mutants indicating that patterning of brain and notochord are normal (figure S1D). Therefore, MZ *ewsa/ewsa* mutant zebrafish were raised until adulthood. Adult MZ *ewsa/ewsa* mutant zebrafish displayed protruding jaws and curved spines. To further investigate the morphological changes in MZ *ewsa/ewsa* mutant zebrafish, the skeletal elements were visualized with alizarin red staining by a Leica DFC320 camera attached to a Leica MZ FLIII dissecting microscope. The dentary (the dermal bone that

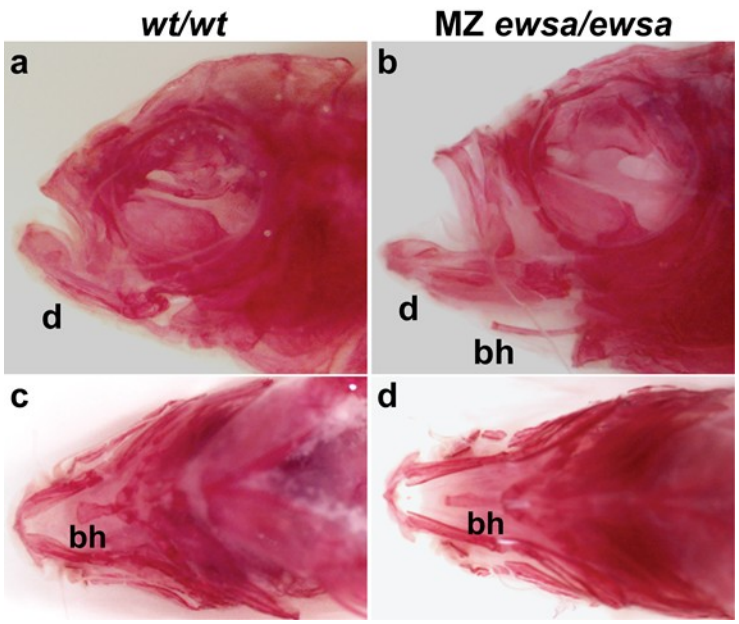

Figure 2: Craniofacial bone defects observed in MZ *ewsa/ewsa* mutant zebrafish

Alizarin red staining of adult zebrafish, anterior is to the left in all images. (a-b) Lateral views of lower jaws showing a typical *wt/wt* fish (a), the protruding jaw commonly found in the MZ *ewsa/ewsa* mutant fish (b), and the protruding basihyal found in MZ *ewsa/ewsa* mutants (b). (c-d) Ventral views of lower jaws of *wt/wt* and MZ *ewsa/ewsa* fish respectively showing the elongated slender basihyal bone found in mutants compared to the flanged basihyal of the wild type. Abbreviations: bh = basihyal, d = dentary.

forms the antero-lateral region of the lower jaw), was pushed upward and anteriorly in adult MZ *ewsa/ewsa* mutants (65%, n=20 fish) compared to adult *wt/wt* zebrafish (0%, n=11 fish) (figure 2b compared to figure 2a). In addition, 40% (n=20) of MZ *ewsa/*ewsa mutants had ventral craniofacial bones extended abnormally far ventrally and the basihyal bones projected anteriorly below the lower jawline (figure 2b), and this did not occur in *wt/wt* zebrafish (0%, n=11). In higher numbers of mutants (70%, n=20), the basihyal was also elongated and straight (figure 2d) compared to the more often flanged bones of the *wt/wt* zebrafish (36%, n=11) (figure 2c).

To determine when the MZ *ewsa/ewsa* mutants start displaying skeletal defects, the chondrocytes of *wt/wt* and MZ *ewsa/ewsa* mutants at 2 to 9 dpf were visualized using alcian blue staining. There were no phenotypic differences between *wt/wt* and MZ *ewsa/ewsa* mutants at 3 dpf. At 4 dpf, the MZ *ewsa/ewsa* mutants displayed an aberrantly angled Meckel's cartilage (m) compared to *wt/wt* embryos (figure 3b and 3a respectively). Photographs of embryos from a lateral view were taken, and the angle formed by the Meckel's cartilage and palatoquadrate

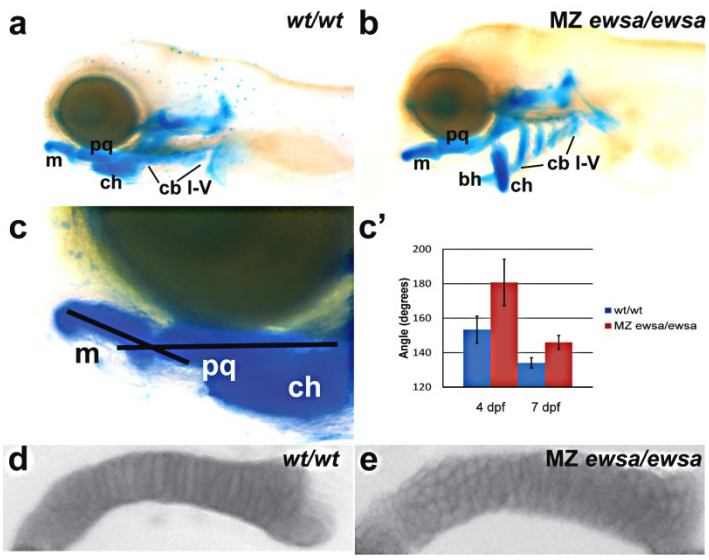

Figure 3: Craniofacial cartilage defects in MZ *ewsa/ewsa* mutants

(a-b) Lateral views of 4 dpf embryos stained with alcian blue. (a) Shows a typical wild type embryo. (b) Shows mutant craniofacial cartilage misalignment. (c) Close up of Meckel's cartilage and palatoquadrate demonstrating the jawbone angle measurements taken. (c') Graphical representation of jawbone angle measurements comparing wild type to mutant at 4 and 7 dpf. (*wt/wt* n= 28 and 5 at 4 and 7 dpf respectively; MZ *ewsa/ewsa* n=32 and 14 at 4 and 7 dpf respectively; error bars represent mean ± standard deviation). (d-e) Alcian blue stained, dissected, and flat mounted Meckel's cartilages of 4 dpf wild type and mutant embryos respectively, showing the smaller, misaligned, more numerous cells of the mutants.

(pq) were measured (figure 3c). As a result, the average angle in MZ *ewsa/*ewsa mutants was wider than *wt/wt* (4 dpf MZ *ewsa/*ewsa mutants: 181^{o} (± 14^{o}), 4 dpf *wt/*wt: 153^{o} (± 8^{o}), 7 dpf MZ *ewsa/*ewsa mutants: 146^{o} (± 4^{o}), and 7 dpf *wt/wt*: 134^{o} (± 3^{o})) (figure 3c'). We also found that the ventral cartilages in 44% (n=32) of MZ *ewsa/ewsa* mutants localized abnormally far downward, whereas none of the *wt/wt* (n=28 embryos) displayed the phenotype (figure 3b). To further analyze the cell morphology, the embryos were microdissected and the craniofacial cartilages were flat mounted. The Mecekl's cartilage of MZ *ewsa/ewsa* embryos contained smaller and increased numbers of cells compared to *wt/wt*. In addition, cells in *wt/wt* cartilages are long and were aligned perpendicular to the long axis. Whereas, the majority of cells in MZ *ewsa/ewsa* embryo cartilages were round and smaller with disorganized alignment (figure 3d-e showing *wt/wt* and MZ *ewsa/*ewsa respectively). This was observed in the Meckel's cartilages of all embryos dissected (100%, n=6) as well as in the ethmoid plates (100%, n=4) and to a lesser extent in the palatoquadrates (33%, n=6) and the ceratohyals (50%, n=6), but not in the ceratobranchials (0%, n=6). These results indicate that Ewsa plays a role in craniofacial bone

development by defining the cell size and alignment of chondrocytes and mesenchymal condensations.

MZ *ewsa/ewsa* mutation leads to axial skeleton abnormalities

The axial skeleton in MZ *ewsa/ewsa* mutant zebrafish visualized with alizarin red staining also displayed high incidence of aberrant neural spines and supraneurals. There was an increased incidence of anterior-posteriorly expanded and widely flanged neural spines (ns) (figure 4b) compared to the sharp spike appearance of neural spines in *wt/wt* fish (figure 4a). The supraneural bone (sn) aligned between the neural spines in *wt/wt* fish, whereas the supraneurals in MZ *ewsa/ewsa* mutant zebrafish are often located dorsal to or fused to the neural spines. In addition, supraneural bones are flat and roughly uniform along the ventral-dorsal axis in *wt/wt* fish. On the other hand, the supraneural bones are irregularly shaped ventral-dorsally and also have projections laterally in the MZ *ewsa/ewsa* mutants (figure 4a and 4b). There were 35% (n=20) of MZ *ewsa/ewsa* mutant fish with misaligned supraneurals, 71% (n=7) of which had one or more fused to the adjacent neural spines (figure 4b). In *wt/wt* fish, the neural arches come back posteriorly across the vertebrae before turning dorsally for the neural spines. In MZ *ewsa/ewsa* mutants, the trunk neural arches and spines are straight as is more common by the caudal vertebrae (figure 5b compared to 5a). One or more hemal spines were also irregularly shaped having bifurcations or kinks in 75%

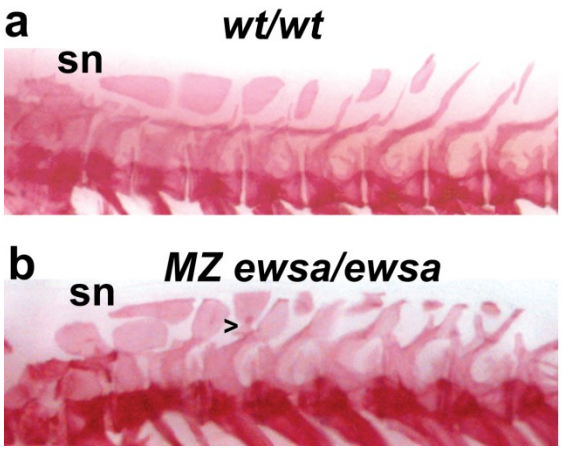

Figure 4: MZ *ewsa/ewsa* mutants have aberrant dorsal elements

Lateral view of first ten vertebrae in adult fish, visualized with alizarin red staining, anterior is to the left and dorsal is up. (a) Typical wild type (b) Mutant displaying aberrant phenotypes observed in dorsal elements. > pointing to supraneural 5 fused to neural spine 5. Abbreviations: sn = supraneural.

(n=20) of MZ *ewsa/ewsa* zebrafish. In eleven wild type fish, one bifurcated hemal spine and one bent hemal spine were observed (9%, n=11). Additionally, the centrums of many caudal vertebrae were asymmetrical, and the intervertebral discs were reduced in MZ *ewsa/ewsa* mutants (figure 5d compared to 5c). We measured the distance between caudal vertebrae and found the average intervertebral space to be 63μm (± 29μm) in MZ *ewsa/ewsa* mutant zebrafish (n=216) and 82μm (± 33μm) in *wt/wt* zebrafish (n=143) (figure 5e). This showed statistical significance by a Welch's t-test with p=0.00000005. These defects lead to curved spines in 40% (n=20) of MZ *ewsa/ewsa* mutants (figure 5b). All of the spines of *wt/wt* fish were normal (n=11) (figure 5a).

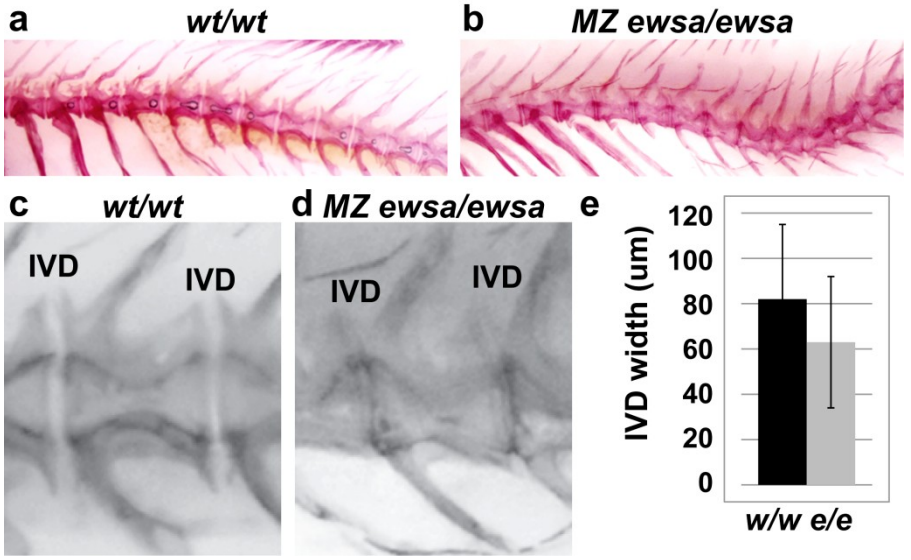

Figure 5: MZ *ewsa/ewsa* mutants have reduced intervertebral discs and curved spines

(a-b) Lateral views of middle vertebrae in *wt/wt* and MZ *ewsa/ewsa* mutant adult zebrafish respectively, visualized with alizarin red staining, anterior is to the left and dorsal is up. (c-d) Magnified images of representative intervertebral discs in *wt/wt* and MZ *ewsa/ewsa* mutants respectively. (e) Graphical representation of invertebral space measurements. Error bars signify means ± standard deviations.

To further specify the stage when defects in vertebrae starts, we performed immunohistochemistry using anti collagen II antibodies at 27 hpf to 3 dpf embryos. There are no significant differences of collagen II protein localization between *wt/wt* and MZ *ewsa/ewsa* mutants at 27 hpf. At 36 hpf, MZ *ewsa/ewsa* mutants displayed bigger, higher numbers, and stronger intensity collagen II signals compared to *wt/wt* zebrafish. In addition, collagen II signals were also prominent in the

notochord extension of MZ *ewsa/ewsa* mutants. Whereas, *wt/wt* zebrafish have less distinct notochord extension with reduced Collagen II signals (figure 6). It is noteworthy that there were no significant differences of notochord lengths (table S1), and also the localization of Collagen II at the caudal fin between *wt/wt* and MZ *ewsa/ewsa* mutants (figure S2). These data suggest that Ewsa regulates the expression of Collagen II at the notochord and the notochord extension.

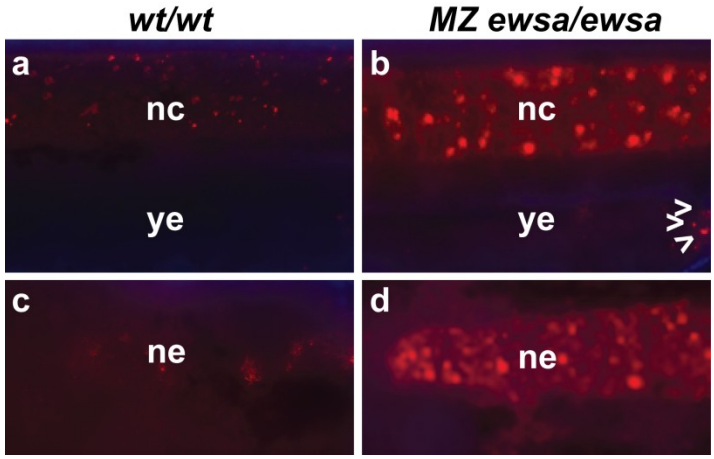

Figure 6: MZ *ewsa/ewsa* mutants have increased Collagen II localization at 36 hpf

Notochords of 36 hpf embryos visualized by immunohistochemistry using an anti-Collagen II antibody. (a-b) 20x magnification of notochords midway along the embryos showing increased Collagen II localization at the notochord of MZ *ewsa/ewsa* mutants above the yolk sac extension. > points to signal localized at the tip of the yolk sac extension in mutants. (c-d) 20x magnification of notochord extensions showing increased localization in MZ *ewsa/ewsa* mutants. Abbreviations: nc = notochord, ne = notochord extension, ye = yolk sac extension.

Ewsa interacts with Sox9 and regulates its target genes

Most of the craniofacial bones develop endochondrally replacing the cartilages seen in figure 3. These craniofacial cartilages are neural crest derived tissues (Noden, 1983; Kague, 2012). As such, they are under transcriptional regulation by Sox9 (Cheung, 2003; Lee, 2004). Sox9 has also been shown to be important for cartilage morphogenesis, endochondral ossification, and collagen II expression (Lefebvre, 1997; Bi, 1999; Yan, 2002; Akiyama, 2002; Dale, 2011). As the axial also develops endochondrally (Arratia, 2001), a commonality between the different phenotypes observed is Sox9 transcriptional regulation. Ews has been shown to be a transcriptional modulator (Rossow,

2001; Araya, 2003, 2005; Li, 2010). Therefore, we hypothesized that EWS directly interacts with SOX9 and modulates its target genes during skeletogenesis.

To determine whether EWS interacts with SOX9, we transfected a FLAG tagged-SOX9 DNA construct into HeLa cells. The cell lysates were extracted, and it was subjected to immunoprecipitation using an anti-FLAG antibody followed by western blotting using an anti-EWS antibody. The coimmunoprecipitation experiment revealed that EWS is precipitated with SOX9, and it indicates the biochemical interaction between EWS and SOX9 (figure 7). This data suggests that EWS may directly regulate Sox9 activity.

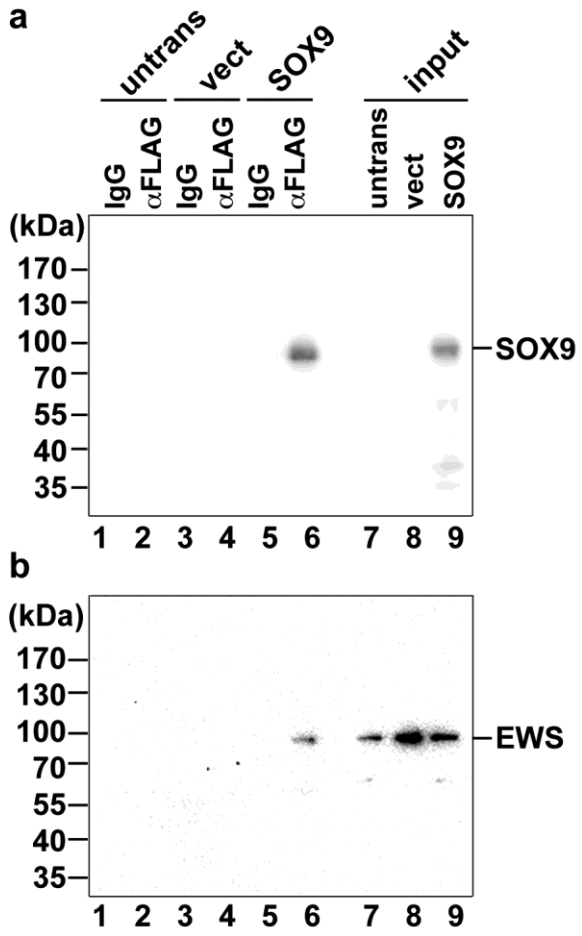

Figure 7: EWS immunoprecipitates with SOX9

Western blot detection of proteins after coimmunoprecipitation with anti-FLAG antibody conjugated dynabeads precipitating FLAG-SOX9. (a) Blot for FLAG-SOX9 showing enrichment of recombinant SOX9 in the precipitate, and lack of signal in the nonspecific control precipitation. (a) Blot for EWS showing that EWS is present in starting lysates, but is only precipitated with SOX9 by the anti-FLAG antibody and not by the control nonspecific antibody.

To address whether the expression levels of Sox9 target genes are changed in the MZ *ewsa/ewsa* mutants compared to *wt/wt*, mRNAs were isolated from 27 hpf embryos that were obtained from both lines, and cDNAs were synthesized using poly T primers. Then, using primers specific to SOX9 target genes, qPCR was performed and relative mRNA expression levels between MZ *ewsa/ewsa* mutants and *wt/wt* embryos were compared. Thirty Sox9 target

genes were selected from a previous report (Table S2) (Oh, 2010). Among these genes, we found that *Sox5, Noggin1, Noggin2,* and *Bmp4* are downregulated while *Ctgfa, Ctgfb, Col2a1a, and Col2a1b* are upregulated in MZ *ewsa/ewsa* mutants relative to *wt/wt* (figure 8). Relative expression levels and p-values calculated by a two-tailed student's t test are listed in table 1. This data suggests that Ews regulates the mRNA levels of SOX9 target genes. Together with the data showing interaction between EWS and SOX9, it suggests that EWS regulates SOX9 transcriptional regulatory activity, and by this mechanism, regulates skeletogenesis.

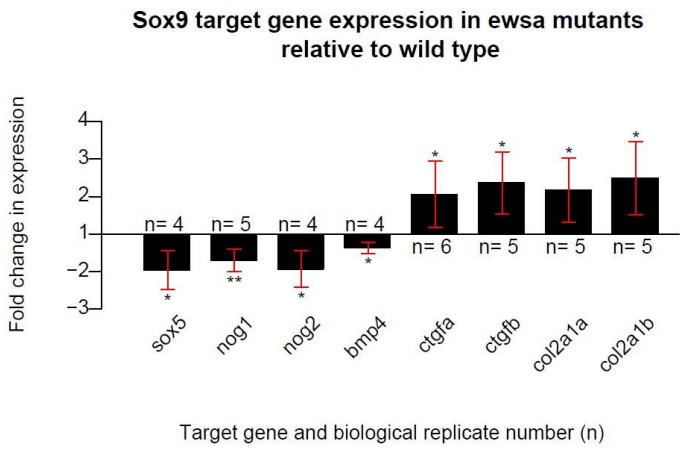

Figure 8: SOX9 target genes have altered expression levels in MZ *ewsa/ewsa* mutants

Barplot showing eight SOX9 target genes with significant fold change in expression relative to wild type embryos at 27 hpf. * p<0.05, ** p<0.01

Table 1: Relative fold gene expression in MZ *ewsa/ewsa* mutants compared to wild type

Target mRNA	Relative Fold Expression	p-value
Sox5	-2.0	0.03
Nog1	-1.7	0.006
Nog2	-1.9	0.03
Bmp4	-1.4	0.01
Ctgfa	+2.1	0.03
Ctgfb	+2.4	0.02
Col2a1a	+2.2	0.04
Col2a1b	+2.5	0.03

DISCUSSION

We identified eight SOX9 target genes are either upregulated (*ctgfa, ctgfb, col2α1a, col2α1b*) or downregulated (*sox5, nog1, nog2, bmp4*) in the *MZ ewsa/ewsa* mutant compared to the *wt/wt* zebrafish embryos. Together with the biochemical interaction between Sox9 and EWS (figure 7), we propose that EWS regulates skeletogenesis through modulating the transcriptional regulation activity of SOX9. This is the first demonstration of molecular function of EWS in skeletogenesis. Because a co-immunoprecipitation (IP) experiment only provides the information of the interaction ability between/among molecules, it is still unclear whether the EWS and SOX9 complex localizes on the chromatin structure and directly regulates transcription, or the complex localizes off the chromatin and thereby regulating the SOX9 protein levels that are recruited to chromatin. Previous reports have shown that EWS associates with p300 and regulates chromatin structure (Rossow, 2001). In addition, other reports have shown that SOX9 associates with p300 and regulate its target genes (Tsuda, 2003; Furumatsu, 2005). Based on these reports, it is conceivable that EWS, SOX9, and p300 form a complex or EWS/p300 and SOX9/p300 heterodimers compete for target loci. Alternatively, it is also possible that EWS and SOX9 form a heterodimer and regulate SOX9 target genes either on chromatin or on non-chromatin sites. In future studies, it will be critical to examine the DNA binding activity of these possible dimers or complexes, and their affect on transcriptional activity of SOX9 target genes.

The craniofacial skeletal defects in MZewsa/ewsa mutants can be explained by multiple possibilities. The craniofacial bone cell morphology is reminiscent of what is seen in endochondral bones of mice mutant for *sox5* and *sox6* (smits, 2001). In their mouse model, the chondrocyte differentiation pathway is errant resulting in chondroblasts which poorly differentiate and mature in a disordered pattern. This leads to cells that fail to form regular columnar shapes and fail to stack orderly. Sox5 and Sox6 transcription factors work

cooperatively with Sox9 in the chondrocyte differentiation pathway (Akiyama, 2002). The expression level of *sox5* mRNA was reduced in the MZ ewsa/ewsa mutant compared to the wt/wt zebrafish embryos. This reduction of *sox5* expression may contribute to the mispolarized and non-columnar cells in the MZ *ewsa/ewsa* mutant craniofacial bones. Second, craniofacial skeletal defects in MZewsa/ewsa mutants may be due to failure in cell migration. Cell migration is a critical step for skeletogenesis, and mesenchymal condensations and developing cartilages must move into the correct position for bone deposition. During this process, cellular adhesions and extra cellular matrix remodeling have to be tightly regulated. We discovered that the mRNA expression levels of both zebrafish *connective tissue growth factor* homologues (*ctgfa* and *ctgfb*) are upregulated in MZ *ewsa/ewsa* mutants. Ctgf is an important secreted molecule which enhances cell adhesion of chondrocytes (Hoshijima, 2006). Based on this, it is conceivable that upregulation of Ctgfa and Ctgfb lead to increased cellular adhesion in the developing cartilages of MZ ewsa/ewsa mutant. And it ultimately may inhibit their migration and lead to a protruding jaw.

The development of the supraneural bones and neural spines is not well understood beyond that they develop endochondrally from scleratomal cells (Deutsch, 1988; Watanabe, 1998; Aoyama, 2000; Arratia, 2001), and it is patterned by antagonizing *noggin* and *bmp4* signals and *hox* gene expression. The MZ *ewsa/ewsa* mutant displayed reduced expression of *noggin* and *bmp4*. It has been shown in a mouse model of campomelic dysplasia, that Sox9 is expressed at the growth plates of vertebrae and in the intervertebral discs (Henry, 2012). In these mice, vertebral growth plates arrested and intervertebral discs compressed after induction of Sox9 knockout. This also leads to increased apoptosis in the vertebrae and severe kyphosis. In addition to asymmetrical vertebral centrums, we report that MZ *ewsa/ewsa* mutants also have reduced intervertebral disks. It stands to reason that because known patterning targets of Sox9

transcriptional regulation (*noggin* and *bmp4*) are misregulated, altered Sox9 activity due to Ews loss could lead to the axial skeletal defects including the curved spines.

Among the identified misregulated SOX9 target genes in the MZ ewsa/ewsa mutant, it is significant to further elucidate which gene(s) misregulation is responsible for the defects in craniofacial bone, or in spine and misdifferention of notochord extension. All of the genes are expressed in the cranial facial skeleton, spine and notochord extension. Importantly, it is highly possible that these defects are induced by misexpression of either single genes or combinations of multiple genes. Therefore, conducting the knockdown or overexpression experiments for single or combinations of SOX9 target genes in the zebrafish will reveal which skeletal structures may be regulated by particular gene sets. We provide evidence for a novel layer of regulation on SOX9 control of endochondral bone and cartilage development, and the tissue specific role for EWS may provide some insight into the formation of Ewing's Sarcoma.

LITERATURE CITED

Akiyama H, Chaboissier MC, Martin JF, Schedl A, de Crombrugghe B. (2002) *The transcription factor Sox9 has essential roles in successive steps of the chondrocyte differentiation pathway and is required for expression of Sox5 and Sox6*. Genes and Development. Nov 1;16(21):2813-28. PMID: 12414734

Amores A, Force A, Yan Y-L, Joly L, Amemiya C, Fritz A, Ho RK, Langeland J, Prince V, Wang Y-L, Westerfield M, Ekker M, Postlethwait JH. (1998) *Zebrafish hox Clusters and Vertebrate Genome Evolution*. Science. Nov 27;282(5394):1711-4. PMID: 9831563

Aoyama H, Asamoto K. (2000) *The developmental fate of the rostral/caudal half of a somite for vertebra and rib formation: experimental confirmation of the resegmentation theory using chick-quail chimeras*. Mechanisms of Development. Dec;99(1-2):71-82. PMID: 11091075

Araya N, Hirota K, Shimamato Y, Miyagishi M, Yoshida E, Ishida J, Kaneko S, Kaneko M, Nakajima T, Fukamizu A. (2003) *Cooperative Interaction of EWS with CREB-binding Protein Selectively Activates Hepatocyte Nuclear Factor 4-mediated Transcription*. Journal of Biological Chemistry. Feb 14;278(7):5427-32 PMID: 12459554

Araya N, Hiraga H, Kako K, Arao Y, Kato S, Fukamizu A. (2005) *Transcriptional down-regulation through nuclear exclusion of EWS by PRMT1*. Biochemical and Biophysical Research Communications. Apr 8;329(2):653-60. PMID: 15737635

Arratia G, Schultze H-P, Casciotta J. (2001) *Vertebral Column and Associated Elements in Dipnoans and Comparison With Other Fishes: Development and Homology*. Journal of Morphology. Nov;250(2):101-72. PMID: 11746457

Azuma M, Toyama R, Laver E, Dawid IB. (2006) *Perturbation of rRNA Synthesis in the bap28 MutationLeads to Apoptosis Mediated by p53 in the Zebrafish Central Nervous System.* Journal of Biological Chemistry. May 12;281(19):13309-16. PMID: 16531401

Azuma M, Embree LJ, Sabaawy H, Hickstein DD. (2007) *Ewing Sarcoma Protein Ewsr1 Maintains Mitotic Integrity and Proneural Cell Survival in the Zebrafish Embryo*. PLoS ONE Oct 3;2(10):e979. PMID: 17912356

Bagnall KM, Higgins SJ, Sanders EJ. (1988) *The contribution made by a single somite to the vertebral column: experimental evidence in support of resegmentation using the chick-quail chimaera model*. Development. May;103(1):69-85.

Bi W, Deng JM, Zhang Z, Behringer RR, de Crombrugghe B. (1999) *Sox9 is required for cartilage formation*. Nature Genetics. May;22(1):85-9. PMID: 10319868

Bi W, Huang W, Whitworth DJ, Deng JM, Zhang Z, Behringer RR, de Crombrugghe B. (2001) *Haploinsufficiency of Sox9 results in defective cartilage primordial and premature skeletal mineralization*. PNAS. Jun 5;98(12):6698-703. PMID: 11371614

Cheung M, Briscoe J. (2003) *Neural crest development is regulated by the transcription factor Sox9*. Developmental Neurobiology. Dec;130(23):5681-93. PMID: 14522876

Cho J, Shen H, Yu H, Li H, Cheng T, Lee SB, Lee BC. (2011) *Ewing sarcoma gene Ews regulates hematopoietic stem cell senescence*. Blood. Jan 27;117(4):1156-66. PMID: 21030557

Dale RM, Topczewski J. (2011) *Identification of an evolutionarily conserved regulatory element of the zebrafish col2a1a gene*. Developmental Biology. Sep 15;357(2):518-31. PMID: 21723274

Delattre O, Zucman J, Melot T, Garau XS, Zucker J-M, Lenoir GM, Ambros PF, Sheer D, Turc-Carel C, Triche TJ, Aurias A, Thomas G. (1994) *The Ewing Family of Tumors – A Subgroup of Small-Round-Cell Tumors Defined by Specific Chimeric Transcripts*. New England Journal of Medicine. Aug 4;331(5): 294-9. PMID: 8022439

Deutsch U, Dressler GR, Gruss P. (1988) *Pax 1, a member of a paired box homologous murine gene family, is expressed in segmented structures during development*. Cell. May 20;53(4):617-25. PMID: 2453291

Eames BF, Yan Y-L, Swartz ME, Levic DS, Knapik EW, Postlethwait JH, Kimmel CB. (2011) *Mutations in fam20b and xylt1 Reveal That Cartilage Matrix Controls Timing of Endochondral Ossification by Inhibiting Chondrocyte Maturation*. PLoS Genetics. Aug;7(8):e1002246. PMID: 21901110

Embree LJ, Azuma M, Hickstein DD. (2009) *Ewing Sarcoma Fusion Protein EWSR1/FLI1 Interacts with EWSR1 Leading to Mitotic Defects in Zebrafish Embryos and Human Cell Lines*. Cancer Research. May 15;69(10):4363-71. PMID: 19417137

Fan C-M, Tessier-Lavigne M. (1994) *Patterning of Mammalian Somites by Surface Ectoderm and Notochord: Evidence for Sclerotome Induction by a Hedgehog Homolog*. Cell. Dec 30;79(7):1175-86. PMID: 8001153

Furumatsu T, Tsuda M, Yoshida K, Taniquchi N, Ito T, Hashimoto M, Ito T, Asahara H. (2005) *Sox9 and p300 cooperatively regulate chromatin-mediated transcription*. Journal of Biological Chemistry. Oct 21;280(42):35203-8. PMID: 16109717

Henry SP, Liang S, Akdemir KC, de Crombrugghe B. (2012) *The Postnatal Role of Sox9 in Cartilage*. Journal of Bone and Mineral Research. Dec;27(12):2511-25. PMID: 22

Javidan Y, Schilling TF. (2004) "Development of Cartilage and Bone" *The Zebrafish: 2nd Edition Cellular and Developmental Biology.* Methods in Cell Biology. Ed. Detrich III HW, Westerfield M, Zon LI. Vol. 76:415-436. ISBN: 0-12-564171-0

Johnson RL, Laufer E, Riddle RD, Tabin C. (1994) *Ectopic expression of Sonic hedgehog alters dorsal-ventral patterning of somites*. Cell. Dec 30;79(7):1165-73. PMID: 8001152

Kague E, Gallagher M, Burke S, Parsons M, Franz-Odendaal T, Fisher S. (2012) *Skeletogenic Fate of Zebrafish Cranial and Trunk Neural Crest*. PLoS One. Nov 14;7(11):e47394. PMID: 23155370

Karsenty G, Wagner EF. (2002) *Reaching a Genetic and Molecular Understanding of Skeletal Development*. Developmental Cell. Apr;2(4):389-406. PMID: 11970890

Kimmel CB, Ballard WW, Kimmel SR, Ullmann B, Schilling TF. (1995) *Stages of Embryonic Development of the Zebrafish*. Developmental Dynamics. Jul;203(3):253-310. PMID: 8589427

Lee Y-H, Aoki Y, Hong C-S, Saint-Germain N, Credidio C, Saint-Jeannet J-P. (2004) *Early requirement of the transcriptional activator Sox9 for neural crest specification in Xenopus*. Developmental Biology. Nov 1;275(1):93-103. PMID: 15464575

Lefebvre V, Huang W, Harley VR, Goodfellow PN, de Crombrugghe B. (1997) *SOX9 is a potent activator of the chondrocyte-specific enhancer of the alpha1(II) collagen gene*. Molecular and Cellular Biology. Apr;17(4):2336-46. PMID: 9121483

Li H, Watford W, Li C, Parmelee A, Bryant MA, Deng C, O'Shea J, Lee SB. (2007) *Ewing sarcoma gene EWS is essential for meiosis and B lymphocyte development*. Journal of Clinical Investigation. May;117(5):1314-23. PMID: 17415412

Li Y, Dudley AT. (2009) *Noncanonical frizzled signaling regulates cell polarity of growth plate chondrocytes*. Development. Apr;136(7):1083-92. PMID: 19224985

Li X, McGee-Lawrence ME, Decker M, Westendorf JJ. (2010) *The Ewing's Sarcoma Fusion Protein, EWS-FLI, Binds Runx2 and Blocks Osteoblast Differentiation*. Journal of Cellular Biochemistry. Nov 1;111(4):933-43. PMID: 20665663

McMahon JA, Takada S, Zimmerman LB, Fan C-M, Harland RM, McMahon AP. (1998) *Noggin-mediated antagonism of BMP signaling is required for growth and patterning of the neural tube and somite*. Genes & Development. May 15;12(10):1438-52. PMID: 9585504

Monsoro-Burq A-H, Duprez D, Watanabe Y, Bontoux M, Vincent C, Bricknell P, Le Douarin N. (1996) *The role of bone morphogenetic proteins in vertebral development*. Development. Nov;122(11):3607-16. PMID: 8951076

Neuhauss SCF, Solnica-Krezel L, Schier AF, Zwartkruis F, Stemple DL, Malicki J, Abdelilah S, Stainer DYR, Driever W. (1996) *Mutations affecting craniofacial development in zebrafish*. Development. Dec;123:357-67. PMID: 9007255

Noden DM. (1983) *The role of neural crest in patterning of avian cranial skeletal, connective, and muscle tissues*. Developmental Biology. Mar;96(1):144-65. PMID: 6825950

Oh C-d, Maity SN, Lu J-F, Zhang J, Liang S, Coustry F, de Crombrugghe B, Yasuda H. (2010) *Identification of Sox9 Interaction Sites in the Genome of Chondrocytes*. PLoS One. Apr 9;5(4):e10113. PMID: 20404928

Peters H, Wilm B, Sakai N, Imai K, Maas R, Balling R. (1999) *Pax1 and Pax9 synergistically regulate vertebral column development*. Development. Dec;126(23):5399-408. PMID: 10556064

Postlethwait JH, Yan Y-L, Gates MA, Horne S, Amores A, Brownlie A, Donovan A, Egan ES, Force A, Gong Z, Goutel C, Fritz A, Kelsh R, Knapik E, Liao E, Paw B, Ransom D, Singer A, Thomson M, Abduljabbar TS, Yelick P, Beier D, Joly J-S, Larhammar D, Rosa F, Westerfield M, Zon LI, Johnson SL, Talbot WS. (1998) *Vertebrate genome evolution and the zebrafish gene map*. Nature Genetics. Apr;18(4):345-9. PMID: 9537416

Remak R. (1855) *Untersuchungen über die Entwicklung der Wirbelthiere*. Berlin: Reimer

Rossow KL, Janknecht R. (2001) *The Ewing's Sarcoma Gene Product Functions as a Transcriptional Activator*. Cancer Research. Mar 15;61(6):2690-5. PMID: 11289149

Sanchez G, Bittencourt D, Laud K, Barbier J, Delattre O, Auboeuf D, Dutertre M. (2008) *Alteration of cyclin D1 transcript elongation by a mutated transcription factor up-regulates the oncogenic D1b splice isoform in cancer*. PNAS. Apr 22;105(16):6004-9. PMID: 18413612

Schmittgen TD, Livak KJ. (2008) *Analyzing real-time PCR data by the comparative C_T method*. Nature Protocols. June 5;3(6):1101-8. PMID: 18546601

Talbot JC, Johnson SL, Kimmel CB. (2010) *hand2 and Dlx genes specify dorsal, intermediate and ventral domains within zebrafish pharyngeal arches*. Development. Aug 1;137(15):2507-17. PMID: 20573696

Tirode F, Laud-Duval K, Prieur A, Delome B, Charbord P, Delattre O. (2007) *Mesenchymal Stem Cell Features of Ewing Tumors*. Cancer Cell. May;11(5):421-9. PMID: 17482132

Tsuda M, Takahashi S, Takahashi Y, Asahara H. (2003) *Transcriptional co-activators CREB-binding protein and p300 regulate chondrocyte-specific gene expression via association with Sox9*. Journal of Biological Chemistry. Jul 18;278(29):27224-9. PMID: 12732631

von Ebner V. (1888) Urwirbel und Neugliederung der Virbelsäule. sitzungsber. Akad. Wiss. Wien III/97, 194-206.

Walker MB, Kimmel CB. (2007) *A two-color acid-free cartilage and bone stain for zebrafish larvae*. Biotechnic & Histochemistry. Feb;82(1):23-8. PMID: 17510811

Watanabe Y, Duprez D, Monsoro-Burq A-H, Vincent C, Le Douarin NM. (1998) *Two domains in vertebral development: antagonistic regulation by SHH and BMP4 proteins*. Development. Jul;125(14):2631-9. PMID: 9636078

Yan Y-L, Miller CT, Nissen RM, Singer A, Liu D, Kirn A, Draper B, Willoughby J, Morcos PA, Amsterdam A, Chung B-c, Westerfield M, Haffter P, Hopkins N, Kimmel C, Postlethwait JH. (2002) *A zebrafish sox9 gene required for cartilage morphogenesis*. Development. Nov;129(21):5065-79. PMID: 12397114

SUPPLEMENTAL TABLES AND FIGURES

Table S1: wt/wt and MZ ewsa/ewsa embryos grow at similar rates based on notochord length

age (days post fertilization)	wt/wt notochord length (± s.d.):	MZ ewsa/ewsa notochord length (± s.d.):	n (wt,mutant)
2	2.73 (± 0.07)	2.71 (± 0.05)	(6,4)
3	3.43 (± 0.08)	3.27 (± 0.07)	(11,11)
4	3.64 (± 0.10)	3.52 (± 0.09)	(8,11)
6	3.69 (± 0.07)	3.62 (± 0.07)	(11,8)
7	3.74 (± 0.09)	3.70 (± 0.12)	(11,8)

Table S2: Primer sequences used in qPCR analysis.

Target	Forward Primer (5'-3')	Reverse Primer (5'-3')
Cata1	GGGATCCCAAGAGTTTGGAG	GATGGACCTTTGTTGCTGGAG
Cata2	GACGAGCGCTACGTCCCC	CTGTGTGACCAGCGGCTCC
Bmp4	CCTGGTAATCGAATGCTGATG	CGCTTTCTTCTTCCCTTCCTC
Ctsb	CGGCTGGCGTTCCTGTGTG	GACCATCTCATGGGACAAGG
Col1a1a	GCTTTGTGGATATTCGGCTGG	CCAATGTGCAGCTGCCGCC
Col2a1a	GCTGGATTCACGGACTCTCC	CCTTTGCACCAAGTGACCGG
Col2a1b	GGAGCAAGACCCCGGCGG	GCCGCTGTCACACACACAG
Col9a2	GCTGAGTTCTTCATCGTCCTC	CAGCGGGGCCTTGAGCTC
Col11a1a	GAGAGGCCAAGGTGGTCCC	CCTGCAGAACCAGGACGAG
Col11a1b	GTGGTCCACGAGATGGAAAAC	GCTCTCACTTGTGTTGCCTG
Col11a2	GATATTCGGAAGAAGCGGAGG	CGCAAAACATCTACTGGATCTG
Ctgfa	GTGTGATTGCTCTGCTGTTCC	GGTGAACACTGGGGCGGC
Ctgfb	CTGGAACAGCATTCACCAGAG	CTCGTCTGGGCAATCACAGG
Epyc	CTCCCCCGAGATACGTCCG	CCTCGTAGGCATTGTCGCC
Erk1	GCGGAATCGGGCAGTAGCG	CGCTTGGTCCCCCAGGTG
Fmoda	GCGGCTAATTGCTCTCCTGC	CATAACCCCGGCTGTGTAAAG
Grb10a	CCTTAGCTGGATGTCCAGAC	GGATGGTCTGTGAGATGAGG
Igf2r	GTCGTGTTGGATTTTGCGGAG	GGCTGTCATCCGAAGCCGC
IL1	GCATGCGGGCAATATGAAGTC	GCGGATCTGAACAGTCCATC
Lef1	CGCAGTTGTCAGGTGGAGG	GCTCCTTGTGCGGGTCTCC

Matn4	GTGTTGGTGTATGTCAGTGTG	GTCAACCGGGCCAGATTTAC
Nog1	GTTTGCTGTCCGCGTACTTG	GCTCCAGCAGGGGTAAAGTG
Nog2	CTACTGCTGCTCCTGTGCG	CTCGATGAGGTCTGGGACG
Ptch1	CTCGGCTGTTAATGTCTCCTC	CGATAGTTGCCCCTATTTCTC
Ptch2	GCCGCCTGTGAACTCAGATC	CTTTCTGTCCCACAGCTTTCC
Prkacaa	GCCAAGAACAAGGGCAATGAG	CAGTGTTCTGTGCTGGGTTC
Prkacab	GGGGCAACGAAATGGAAAGC	CCAGGCAGGCGGTGTTCTG
Prelp	GCTGGGCTTGCATACTGCTG	GATGGGCGAACAGGCTTTGG
Runx2b	CATTCCCGTAGATCCCAGCG	CTGCTGAGGTCCTGCATTCG
Sox5	CTTACTGAGCCTGAGCTTCC	CGTCGCCATGACTACCTCTC
Sox9a	GACCCCTACCTGAAGATGAC	CGCGGAGTCCTCGGACATG
Sox9b	GAAGATGAGTGTGTCCGGAG	GTCTCGCTGTCCGATCCCG
Stat1a	CTCAGTGGTTGGAGCTTCAG	CTGAGATATTGTCGGATGGCC
Stat1b	GCTCTGGAACCAGCTGCAG	GTCGGATCTCCATTGGGAAAG
Sdc3	GCTCCCGTGCTGGATAACG	CTCATCTCCAGAGCTCTCATC
Tgfb3	GCAAAGGACTGCTGTTTGTTC	CAATGTCCACTGTGGTGCAG
Vegfaa	GCGTGCAAGACCCGAGAGC	GCGCATGAGAACCACACAGG
Vegfab	CTTTGCTGTTCGCGTGCTCC	GTGCTTCTGCCTCCCTCTC
Gapdh	CGGATTCGGTCGCATTGGC	GGTCATTGATGGCCACGATC

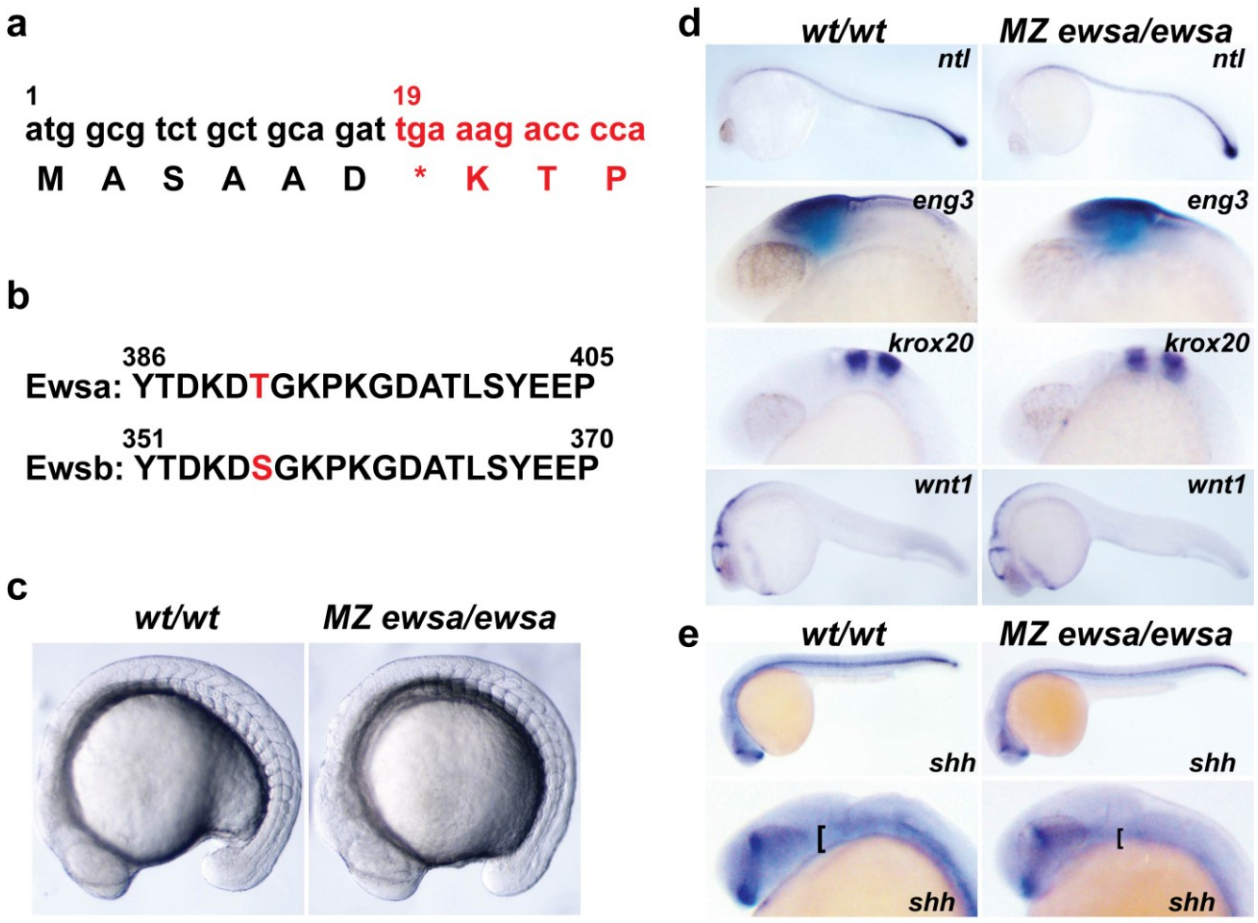

Figure S1: MZ ewsa/ewsa embryos develop normally to 24 hours

(a) Mutated sequence showing a premature stop codon shortly after translation initiation site. (b) Peptide sequences aligned for Ewsa and Ewsb at antigen site for Ewsa antibody. (c) *wt/wt* and MZ *ewsa/ewsa* embryos at 17 somite stage showing normal notochord and somite development. (d) *in situ* hybridization (anterior is to the left) in 24 hpf embryos for *ntl, eng3, krox20,* and *wnt1*. (e) *in situ* hybridization (anterior is to the left) in 24 hpf embryos for *shh*.